

ULTIMATE LOAD CAPACITIES OF PLANE AND AXISYMMETRIC HEADED ANCHORS

By Amy Vogel¹ and Roberto Ballarini²

ABSTRACT: A finite-element-based linear elastic fracture mechanics analysis of the pullout of headed anchors is presented. The anchor is modeled as a vertically loaded crack of diameter c , embedded at a depth d , with a rigid upper surface, and traction-free lower surface. The fracture toughness and Poisson's ratio of the surrounding matrix are K_{Ic} and ν , respectively. For selected values of d/c , the mode-I stress intensity factor is calculated for each increment of the crack growth, which emanates from the edge of the anchor, and follows the direction of zero mode-II stress intensity factor. The stress intensity factors are used to calculate the ultimate load P_u , which is written as $P_u = g(d/c, \nu)d^{3/2}K_{Ic}$. For $\nu = 0.2$ and relatively large values of d/c , $g = 2.8$ for axisymmetric anchors and $g = 1.2$ for plane strain anchors.

INTRODUCTION

Consider a headed anchor of diameter c , embedded within a concrete matrix at a depth d . The formula given in the American Concrete Institute code ("Code" 1989) for its tensile (pullout) capacity can be written, in terms of the concrete tensile strength f_t , as follows:

$$P_u \propto f_t d^2 \quad (1)$$

It is well known (Ozbolt and Eligehausen 1993) that (1), which is based on the assumption that pullout is resisted by a nominal stress acting along an assumed failure surface, is unconservative for relatively large d . This is not surprising, because it is not based on a rational analysis that treats the discrete cracking that dominates the failure process. Over the past 15 years improved design formulas have been developed through linear and nonlinear fracture mechanics; these have been recently summarized by Karihaloo (1996). As discussed by Ozbolt and Eligehausen (1993), for large embedment depths there is very little difference between the predictions of the linear and nonlinear fracture models. Therefore, we limit the subsequent discussion to linear elastic fracture mechanics (LEFM).

Consider the idealized headed anchor geometry shown in Fig. 1. The model consists of an anchor, embedded at a depth $d = 1$, modeled as an infinitesimally thin crack of diameter c , whose upper surface is restrained in all directions and whose lower surface is traction-free. It does not include the thickness of the anchor, nor its stem; these could be easily incorporated but are not expected to significantly affect the ultimate load capacity. The length of the extension from the edge of the anchor is l . A unit load is applied through a prescribed uniform stress along the bottom surface.

In LEFM, it is typically assumed that a crack will propagate when the mode-I stress intensity factor K_I reaches a value equal to the fracture toughness K_{Ic} along a path that is associated with zero mode-II stress intensity factor K_{II} . Linearity and dimensional consistency demand that the load associated with an equilibrium crack length l is of the form

$$P = f(c/d, l/d, \nu)d^{3/2}K_{Ic} \quad (2)$$

¹Dept. of Civ. Engr., Case Western Reserve Univ., Cleveland, OH 44106-7201.

²Prof., Dept. of Civ. Engr., Case Western Reserve Univ., Cleveland, OH.

Note. Associate Editor: Gilles Pijaudier-Cabot. Discussion open until April 1, 2000. To extend the closing date one month, a written request must be filed with the ASCE Manager of Journals. The manuscript for this paper was submitted for review and possible publication on February 2, 1999. This paper is part of the *Journal of Engineering Mechanics*, Vol. 125, No. 11, November, 1999. ©ASCE, ISSN 0733-9399/99/0011-1276-1279/\$8.00 + \$.50 per page. Paper No. 20164.

where ν = Poisson's ratio. The ultimate load corresponds to the crack length that maximizes f ; that is

$$P_u = f_{\max}(c/d, l/d, \nu)d^{3/2}K_{Ic} \equiv g(d/c, \nu)d^{3/2}K_{Ic} \quad (3)$$

Numerical values of g have been presented for plane strain by Ballarini et al. (1985) and for the axisymmetric configuration by Karihaloo (1996) and Eligehausen and Sawade (1989). Eli-

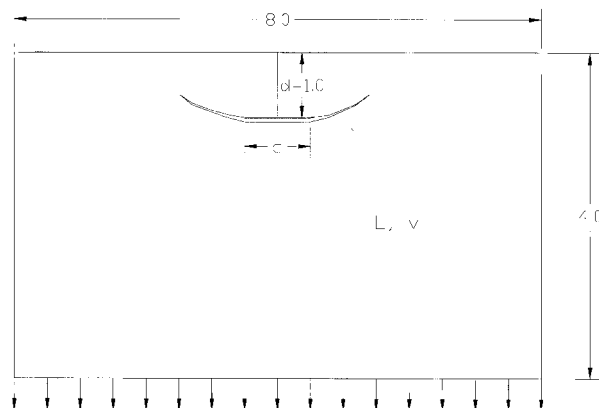


FIG. 1. Schematic of Headed Anchor Bolt Model

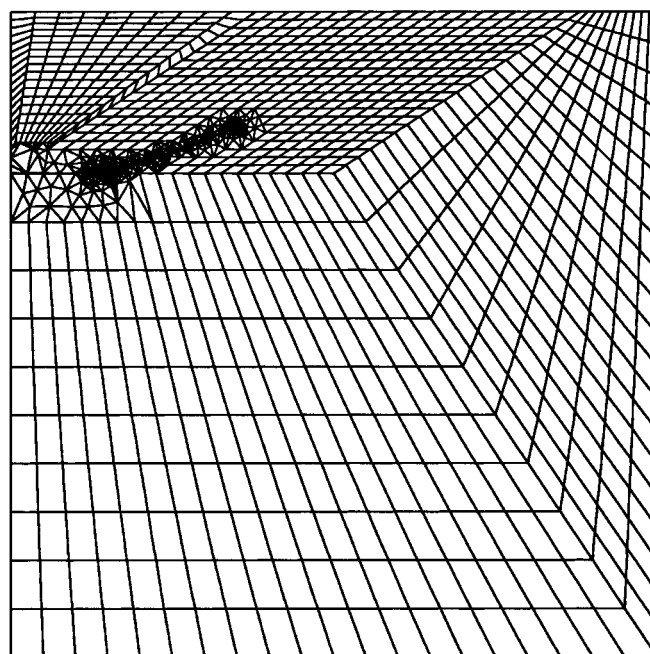


FIG. 2. Finite-Element Discretization of Anchor Bolt Model, $d/c = 1$

gehausen and Sawade (1989), assuming a straight crack propagating at an angle of 37.5° with respect to the plane of the anchor; used the finite-element method to predict that for relatively large embedments $g = 2.1$. More recently Karihaloo (1996), approximating the anchor and failure surface as an embedded penny shaped crack of decreasing depth and increasing radius, calculated that for relatively large embedments $g = 0.6$. The latter result is not surprising, because the constant penny shaped crack is associated with higher stress intensity factors than those at the front of a curving crack. Because of the discrepancy in the published values of g for the axisymmetric configuration, the writers performed an incremental crack growth analysis to calculate improved estimates of functions f and g . By also calculating the results for plane strain conditions, they verified the results presented by Ballarini et al. (1985), which were derived through an approximate crack path analysis.

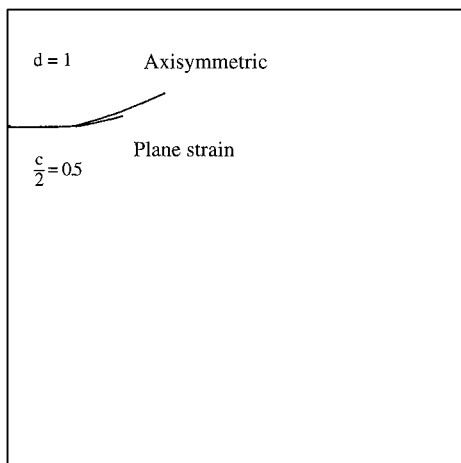


FIG. 3. Crack Paths for Plane Strain and Axisymmetric Configurations, $d/c = 1$

In the subsequent analysis, the local compressive damage that may arise in the vicinity of the anchor is not taken into account. If it were, then the numerical values of g , as well as the cracking patterns, would be dependent on the absolute value of the embedment depth.

FINITE-ELEMENT MODEL

The finite-element program FRANC-2D (1997) was used to model the cracking that develops during the pullout; it possesses automatic remeshing capabilities, accurately calculates the stress intensity factors K_I and K_{II} , and propagates the crack along the zero K_{II} direction. For all calculations, $\nu = 0.2$. Fig. 2 shows a typical finite-element discretization of the original crack and the extension from its edge. Because of symmetry, only the region shown in Fig. 2 needs to be modeled; this region represents half of the geometry for the plane strain configuration and a cross section for the axisymmetric configuration. Recall that the nodes along the top surface of the anchor are restrained in all directions and that zero traction is prescribed on the nodes along the bottom surface. Moreover, symmetry is employed by assigning zero horizontal displacement to all nodes lying along the vertical left bounding surface.

It is important to note that for these (crack surface) boundary conditions, the singularity at the tip of the anchor is not square root; it is oscillatory (Ballarini et al. 1985). Therefore, LEFM cannot be used to predict the crack initiation load. The following procedure is used to initiate the crack. For several values of c , a short crack is introduced at an angle of 30° with respect to the plane of the anchor. This crack is then propagated along a path of zero K_{II} . The arbitrary choice of initiation angle will not significantly affect the predicted g , because under subsequent propagation the crack will redirect itself along the theoretically consistent path.

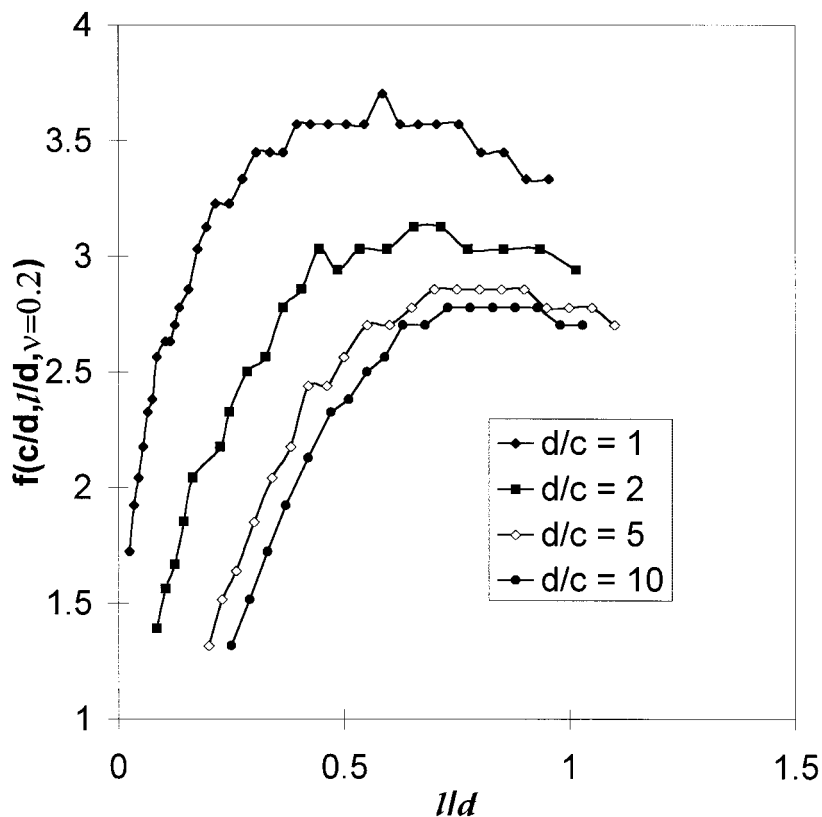


FIG. 4. Normalized Equilibrium Load as Functions of Crack Length and Embedment Depth (Axisymmetric Configuration)

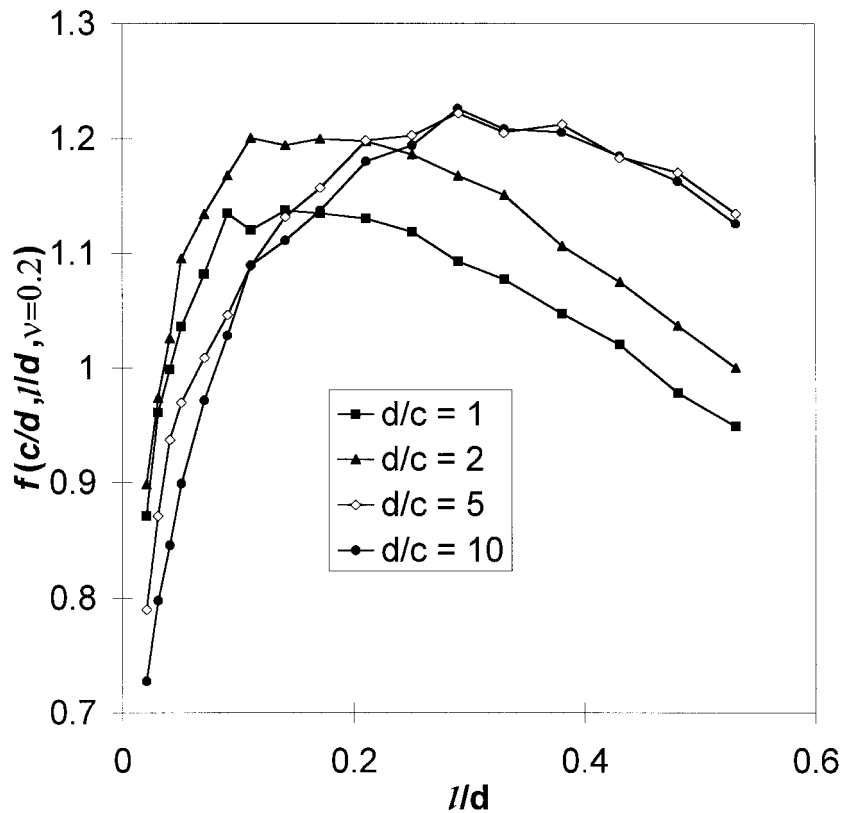


FIG. 5. Normalized Equilibrium Load as Functions of Crack Length and Embedment Depth (Plane Strain Configuration)

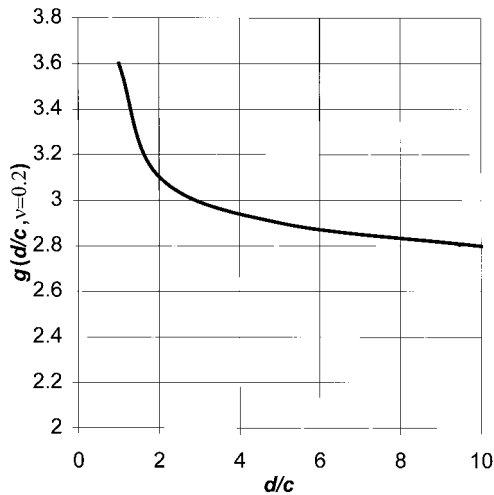


FIG. 6. Normalized Ultimate Load as Function of Embedment Depth (Axisymmetric Configuration)

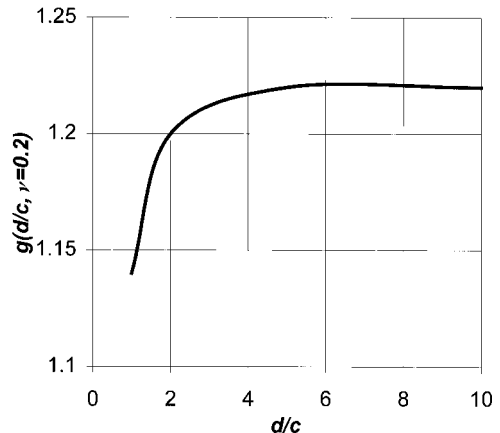


FIG. 7. Normalized Ultimate Load as Function of Embedment Depth (Plane Strain Configuration)

RESULTS AND DISCUSSION

The predicted crack paths for $d/c = 1$ are shown in Fig. 3. Qualitatively, similar paths were calculated for the other embedment depths ($d/c = 2, 5,$ and 10). As will be discussed subsequently, crack propagation in these geometries is stable up to a critical length l_c . It was shown by Ballarini et al. (1985) that for shorter embedment depths ($d/c = 0.75$), crack propagation in the plane strain geometry is unstable at initiation. To capture the ultimate load capacity, each analysis was terminated at a crack length slightly longer than l_c . It is observed that, for each configuration, l_c is longer for axisymmetry than for plane strain. Moreover, the angle of propagation up to the critical length is at most 20° for the axisymmetric configurations and slightly less for the plane strain geometries.

Figs. 4 and 5 show function f ; its maximum value for each configuration provides the nondimensionalized ultimate load

g , as shown in Figs. 6 (axisymmetry) and 7 (plane strain). Although they are not presented, the mode-II stress intensity factors were practically equal to zero for the paths shown in Fig. 3. It is observed that for large values of d/c , g approaches 2.8 for axisymmetry and 1.2 for plane strain. Fig. 7 also shows that, for plane strain, g is a weak function of d/c . In fact, for all practical purposes, function g can be taken as a constant 1.2. The plane strain results for $d/c = 0.75$ and 1.0 agree to two significant figures with those presented by Ballarini et al. (1985).

APPENDIX. REFERENCES

- Ballarini, R., Shah, S. P., and Keer, L. M. (1985). "Failure characteristics of short anchor bolts embedded in a brittle material." *Proc., Royal Soc., London*, A404, 35–54.
- "Code requirements for nuclear safety." (1989). *Appendix B. Steel embedments, manual of concrete practice, Part IV, ACI #349.1R*, ACI Committee 349, American Concrete Institute, Detroit.

Eligehausen, R., and Sawade, G. (1989). "Analysis of anchorage behavior (literature review)." *Fracture mechanics of concrete structures: From theory to applications*, L. Elfgren, ed., Chapman & Hall, London, 263–280.

FRANC-2D. (1997). Cornell Fracture Group Home Page, Cornell University, Ithaca, N.Y.

Karihaloo, B. L. (1996). "Pull-out of axisymmetric headed anchors." *Mat. and Struct.*, 29, 152–157.

Ozbolt, J., and Eligehausen, R. (1992). "Fastening elements in concrete structures—numerical solutions." *Fracture of Concrete and Rock, Proc., 2nd Int. Conf.*, H. P. Rossmanith, ed., E & FN Spon, London, 527–547.